CHAPTER IV

n-OCTANE AROMATIZATION ON Pt-CONTAINING ZEOLITES I. LARGE PORE ALUMINOSILICATE MOLECULAR SIEVES

Siriporn Jongpatiwut, Benjawan Chanajaranwit
Thirasak Rirksomboon, and Somchai Osuwan

The Petroleum and Petrochemical College,
Chulalongkorn University, Bangkok, Thailand

and

Daniel E. Resasco*

School of Chemical Engineering and Materials Science,
The University of Oklahoma, Norman, OK 73019

In progress

Keywords: *n-octane aromatization, Pt/K-LTL, Pt/K-BEA, Pt/K-MAZ, Pt/K-FAU, Pt/SiO*$_2$*, vapor phase impregnation, DRIFTS, catalyst deactivation, TPO, TPD, hydrogen chemisorption*

---

*To whom correspondence should be addressed: e-mail: resasco@ou.edu

ABSTRACT

1% Pt supported on different potassium form of large pore zeolites i.e. Pt/K-LTL, Pt/K-BEA, Pt/K-MAZ, and Pt/K-FAU zeolites were tested for *n*-octane aromatization at 500°C. All catalysts were prepared by vapor phase impregnation (VPI). It was found that Pt/K-LTL catalyst exhibited higher aromatization performance than the other zeolite catalysts. All fresh catalysts were characterized by hydrogen chemisorption, FT-IR of adsorbed CO, and temperature programmed desorption (TPD) of ammonia. It was found that after reduction at either 350 or 500° C, the Pt/K-LTL showed much higher Pt dispersion than other catalysts. In agreement with a previous study, the structure of L zeolite can stabilize the small Pt clusters inside the zeolite channel. FT-IR indicated large fraction of platinum cluster located outside zeolite channel for Pt/K-BEA and Pt/K-MAZ catalysts. After reactions, coke deposit over catalysts were analyzed by temperature programmed oxidation (TPO).

INTRODUCTION

The aromatization of *n*-alkanes is a vital process because of its high valuable aromatic products. It was found that platinum supported on potassium form of L zeolite (Pt/K-LTL) catalysts are highly active and selective for *n*-hexane aromatization [1-3]. The disadvantage of this catalyst is its sensitivity to sulfur [4-6]. There have been a variety of researches studied on the aromatization of *n*-hexane in different aspects e.g. to understand the unique property, reaction pathway [7-13], and to improve the catalyst to withstand the presence of sulfur [14-21]. However, there is much less studies focused on the aromatization of larger chain alkane. Recently, we have investigated the aromatization of *n*-octane over the Pt/K-LTL well-prepared by vapor phase impregnation (VPI) method [22]. We observed unexpected hydrogenolysis aromatic products, which are benzene and toluene. The rapid deactivation due to coke deposit was also found. It is possible that the pore of L-zeolite is too small for both *n*-octane feed and C8-aromatic product molecules.

Therefore, in this contribution, we further studied the aromatization of *n*-octane over other large pore zeolites, which are K-BEA, K-MAZ, and K-FAU and compared to that of K-LTL zeolite. Fresh and spent catalysts were characterized by several techniques e.g. BET, FT-IR of adsorbed CO, hydrogen chemisorption, temperature programmed desorption (TPD) of ammonia, and temperature programmed oxidation (TPO).

EXPERIMENTAL

Catalyst Preparation: The K-LTL-zeolite (KL; Lot#1041, BET area = 292 m^2/g, SiO_2/Al_2O_3 ratio = 6) was produced by Tosoh Co. NaH-BEA (NaHβ; CP810E, Lot#1822-78) and H-MAZ (HΩ; ZD96026, Lot#2163-53-1) zeolites were produced by Zeolyst International. The Na-FAU (NaY; Type Y-54, Lot#955089001010) zeolite was produced by UOP. The formulas and channel systems of the zeolites are listed in Table 1. The precipitated silica Hi-Sil® 233 (CAS# 7631-86-9, BET area =140 m^2/g) was provided by PPG Siam Silica Co., Ltd. NaH-BEA, H-MAZ, and Na-FAU were exchanged three times with 1 M KNO_3 solution in order to ensure the greatest possible elimination of protons. The ion exchange process was carried out at 80°C for 2 h under stirring, using 70 ml per gram zeolite. Prior to addition of the platinum metal, the exchanged zeolites were dried in an oven at 110°C overnight and then calcined in air flow (100ml/min.g_{zeol}) at 400°C for 5 h. The elemental analyses were done by a Varian SpectrAA-300atomic absorption spectroscopy. BET surface areas were also determined by a Quantachrome Autosorb-1. The analysis data in terms of Si/Al, K/Al, and Na including BET area of supports are shown in Table 1. Pt/K-zeolite catalysts were prepared with 1 wt. % Pt by vapor phase impregnation (VPI), whereas Pt/SiO_2 catalyst was prepared by incipient wetness impregnation (IWI) method.

In the IWI method, tetraamineplatinum (II) nitrate (Merck) was weighed and dissolved in deionized water (0.69 cm^3/g support) and then impregnated over the dry support by slowly dropping the solution under a dry-nitrogen atmosphere. Next, the mixture was dried in an oven at 110°C overnight. The cool mixture was loaded into a glass tube and calcined at 350°C in a flow of dry air of 100 cm^3/min.g for 2 h and left to cool to room temperature. The resultant catalyst (Pt/SiO_2) was stored in a desiccator. In the VPI method, the zeolite catalysts were prepared by physically mixing weighed platinum (II) acetylacetonate (Alfa Aesar) and dry support under nitrogen atmosphere. The mixture was then loaded into the reactor tube under a He flow of about 2 cm^3/min. The mixture was slowly ramped to 40°C and held there for 3 h, and ramped again to 60°C and held again for 1 h. After that, further ramped to 100°C, at which temperature the mixture was held for 1 h to sublime the $Pt(AcAc)_2$. After sublimation, the mixture was ramped to 130°C and held for 15 min to ensure that the entire precursor was sublimed. The reactor was cooled to room temperature. After that, it was ramped to 350°C in flow of air for 2 h and calcined at that temperature for 2 h to decompose the Pt precursor. Finally, the catalysts prepared by the VPI method (Pt/K-LTL, Pt/K-BEA, Pt/K-MAZ, and Pt/K-FAU) were stored in a desiccator.

TABLE 1

Formulas and channel structures of different zeolites

Zeolite	**Formula**	**Channel System**[a]
LTL	$K^+_6Na^+_3\ (H_2O)_{27}[Al_9Si_{27}O_{72}]$	**12** 7.1x7.1*
BEA	$Na^+_7[Al_7Si_{57}O_{128}]$	**12** 6.6x6.7**<->[12]5.6x5.6*
MAZ	$Na^+_{10}\ (H_2O)_{28}[Al_{10}Si_{26}O_{72}]$	**12** 7.4x7.4* / [8] 3.1x3.1***
FAU	$Na^+_{58}\ (H_2O)_{24}0[Al_{58}Si_{134}O_{384}]$	**12** 7.4x7.4***

[a]the number of either T- or O-atoms (in bold type) forming the rings controlling diffusion through the channels, and the crystallographic free diameters of the channels in Ångstroem units, based upon the atomic coordinates of the type materials and an oxygen radius of 1.35Å.

The number of asterisks in the notation indicates whether the channel system is one-, two- or three-dimensional. Only those apertures which are more open than regular six-rings have been included. In most cases, the smaller openings simply form windows (rather than channels) connecting larger cavities. Interconnecting channel systems are separated by a double arrow (<->). A vertical bar (|) means that there is no direct access from one channel system to the other. The examples from Table 1 have been selected to illustrate the use of these notations.

Catalytic Activity Measurement: The catalytic activity studies were conducted at atmospheric pressure in a 0.5-inch glass tube with an internal K-type thermocouple for temperature measurement. The reactor was a single-pass, continuous-flow type, with a catalyst bed of 0.20 g. Prior to reaction, the temperature was slowly ramped in flowing H_2 at 100 $cm^3/min.g$ for 2 h up to 500°C and in situ reduced at that temperature for 1 h. *n*-Octane was added by injection from a syringe pump. In all experiments, the hydrogen to *n*-octane molar ratios was kept at 6:1. The products were analyzed in a Shimadzu GC-17A equipped with a capillary HP-PLOT/Al_2O_3 "S" deactivated column, using a temperature program to obtain optimal product separation.

Hydrogen Chemisorption: The amount of adsorbed hydrogen on all fresh catalysts was measured in a static volumetric adsorption Pyrex system, equipped with a high capacity, high vacuum pump that provided vacuum on the order of 10^{-9} torr. Prior to each experiment, 0.4 g of dried fresh catalyst was reduced in situ at 350 and 500°C for 1 h under flowing H_2, cooled down to 300°C, evacuated to at least 10^{-7} torr at 300°C for 20 min, then cooled down to room temperature under vacuum. Adsorption isotherms were obtained with several adsorption points ranging from 0 to 100 torr. The H/Pt values were directly obtained by extrapolating to zero pressure.

Diffuse Reflection Infrared Fourier Transform Spectroscopy (DRIFTS) of Adsorbed CO: The fresh and spent Pt/K-LTL and Pt/SiO_2 catalysts were characterized by DRIFTS using adsorbed CO as a probe in a Nicolet Avatar 360 spectrometer equipped with a DTGS detector. Experiments were performed in a diffuse reflectance cell from Spectra-Tech, type 0030-103 with ZnSe windows. For each IR spectrum, 128 scans were taken at a resolution of 8 cm^{-1}. Prior to taking each spectrum, a background was collected on the sample reduced in situ under a flow of H_2 at 500°C for 1 h and purged in He for 30 min at room temperature. Then, a flow of 3%CO in He for 30 min was sent over the sample, followed by a purge in He flow for 30 min. After this treatment, the spectrum of adsorbed CO was collected.

Temperature Programmed Desorption (TPD) of Ammonia: Temperature programmed desorption of ammonia was carried out using a Micromeritics AutoChem 2910. 50 mg zeolite of zeolite sample that was place in a quartz reactor and heated (3°C/min) under He flow (30 ml/min) up to 550°C for 1 h in order to have a clean catalyst surface. The reactor was cooled down to 100°C, which is adsorption temperature. Then the sample was saturated a flow of 10% NH_3/He (30 ml/min) for 30 min. After purging by He (30 ml/min) for 30 min to eliminate non-adsorbed NH_3 molecules, the sample was heated linearly ramp temperature (10° C/min) to 600°C under the same He flow. The amount of ammonia eluted was analyzed on-line by a TCD detector.

Temperature Programmed Oxidation (TPO): Temperature programmed oxidation was employed to analyze the amount and characteristics of the coke deposits on spent catalysts. The high sensitive TPO system was set up as a previous report [23]. TPO of the spent catalysts was performed in a continuous flow of 2% O_2/He while the temperature was linearly increased at a heating rate of 12°C/min. Before conducting the TPO on a 0.03 g sample placed in a ¼" quartz fixed-bed reactor, the spent catalyst was dried at 110°C overnight and weighed. The catalyst was then flushed by 2% O_2 in He for 30 min before the temperature ramp was started. The CO_2 produced by the oxidation of coke species was further converted to methane by 15%Ni/Al_2O_3 catalyst in the presence of hydrogen at 400°C. The methane obtained was analyzed online by a FID detector. The amount of coke was calibrated by using 100 μl pulses of pure CO_2.

RESULTS

Characterization of Fresh Catalysts: The hydrogen uptake (H/Pt) obtained on the Pt/silica and the Pt/zeolite catalysts after reduced at 350 and 500°C are shown in Table 2. It is clearly seen that for all catalysts, the H/Pt value decreased when the reduction temperature increased. This is due to agglomeration of Pt clusters during reduction at higher temperature. Pt/K-LTL exhibited the highest H/Pt while Pt/K-BEA showed the lowest H/Pt ratio. In agreement with previous studies [24-26], one of the unique properties of Pt/K-LTL for the aromatization of *n*-hexane is the cage structure of L zeolite which is capable to stabilize the small Pt cluster than other zeolites.

TABLE 2

Analysis data of different catalysts and supports

Catalyst	**BET area of support (m^2/g)**	**Si/Al mole ratio**	**K/Al mole ratio**	**H/Pt (after reduced at 350°C)**	**H/Pt (after reduced at 500°C)**
Pt/SiO_2	-	-	-	0.38	0.10
Pt/K-LTL	310	2.79	0.86	1.20	0.75
Pt/K-BEA	657	8.31	1.26	0.24	0.08
Pt/K-MAZ	-	2.36	0.62	0.38	0.12
Pt/K-FAU	1,203	2.12	0.97	0.26	0.22

DRIFTS of Asorbed CO : The DRIFTS of CO adsorbed on Pt/SiO_2, Pt/K-LTL, Pt/K-BEA, Pt/K-MAZ, and Pt/K-FAU are illustrated in Fig.1 As reported previously [19], the adsorption of CO on small Pt cluster inside the L-zeolite channel leads to the formation of Pt carbonyls, which result from a disruption of the Pt clusters by interaction with CO. These Pt carbonyls are stabilized inside L-zeolite channels and exhibit characteristic IR adsorption bands below 2000 cm^{-1}. On the other hand, when the catalyst contains Pt clusters located outside the zeolite channels, a clear shoulders is evident at 2070 cm^{-1}. The band between 2050 and 2000 cm^{-1} were related to CO adsorbed on particles near the pore mouth. Only Pt/K-LTL catalyst exhibited the band below 2000 cm^{-1}, which represents highly disperse Pt inside the zeolite channel. The spectra of adsorbed CO on Pt/K-MAZ and Pt/K-BEA catalysts are centered at 2075 cm^{-1}, which is similar position to that of nonmicroporous Pt/SiO_2 catalysts. Most of spectrum areas are related to the H/Pt values. This would indicate that Pt clusters on K-BEA or K-MAZ are not stabilized by zeolite channel. Therefore, the Pt inside zeolite pore can easily migrate outside and form larger particles under reduction conditions. Strangely, there is no any CO species observed on Pt/K-FAU catalyst.

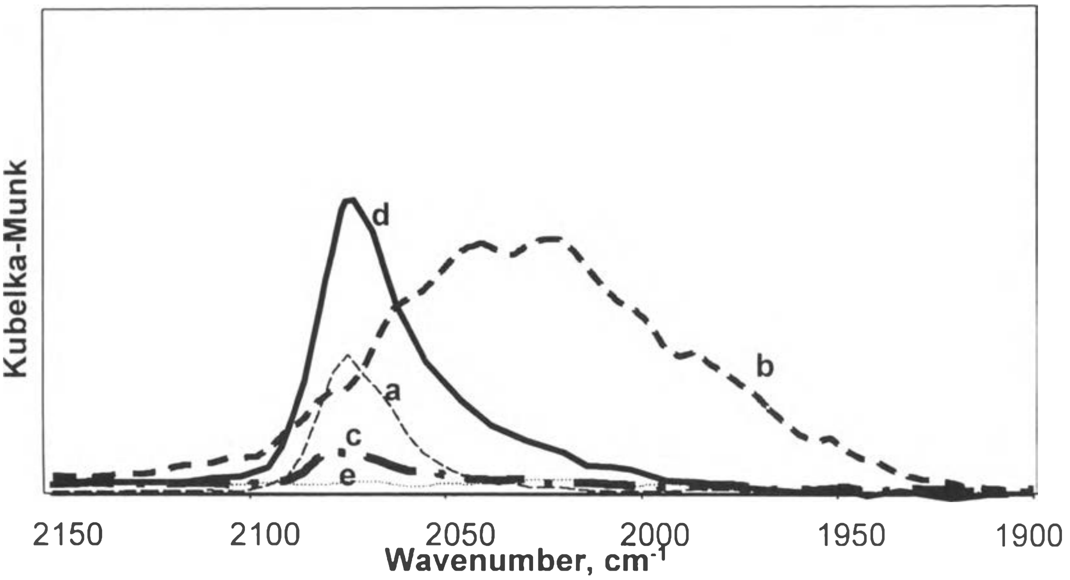

Fig. 1. DRIFTS spectra of CO adsorbed on fresh catalysts reduced in situ at 500°C. The reduced catalysts were exposed to a flow of 3%CO in He for 30 min at room temperature and purged in He for 30 min. (a) Pt/SiO_2, (b) Pt/K-LTL, (c) Pt/K-BEA, (d) Pt/K-MAZ, and (e) Pt/K-FAU.

***TPD of NH_3*:** The TPD profiles of adsorbed ammonia at 100°C on the different catalysts are shown in Fig. 2. Pt/K-BEA, Pt/K-LTL, and Pt/SiO_2 exhibited similar extent of NH_3 adsorbed while Pt/K-MAZ, and Pt/K-FAU showed much higher. All the NH_3 adsorbed were mainly eluted at 180°C. Pt/K-FAU not only exhibited higher acidity but also showed the peak at 330°C. The high-temperature peak represents the acid strength. This would indicate that the high acid strength of FAU could not be removed by common ion-exchanged process.

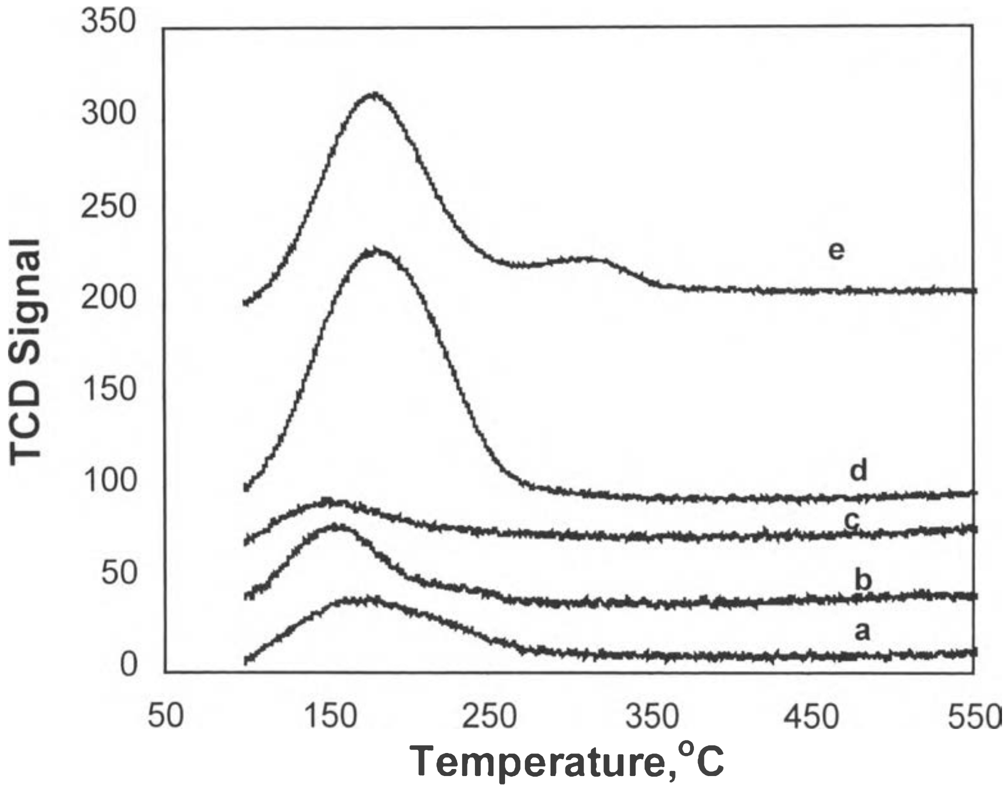

Fig. 2. TPD profiles of ammonia adsorbed on catalyst supports (a) SiO_2, (b) K-LTL, (c) K-BEA, (d) K-MAZ, and (e) K-FAU. The supports were exposed to a flow of 10%NH_3/He at 100°C for 30 min and purged by He for 30 min.

Catalyst Activity Measurement: The Pt/SiO_2, Pt/K-LTL, Pt/K-BEA, Pt/K-MAZ, and Pt/K-FAU catalysts were tested for *n*-octane aromatization at 500°C as a function of time on stream. The *n*-octane conversion and total aromatics selectivity obtained are shown in Fig. 3a and b, respectively. It was observed that the Pt/K-LTL exhibited higher activity and total aromatics selectivity than other zeolite catalysts. However, the activity dropped rapidly at 4 h on stream. In our previous study [22], we have found that the drop is due to pore plugging by coke formation. Pt/K-FAU behaved the same trend but the deactivation was more pronounced. After only few hours on stream, Pt/K-BEA, Pt/K-MAZ, and Pt/K-FAU exhibited lower activity and total aromatics selectivity than nonmicroporous silica catalyst. The product distributions are listed in Table 3. Pt/K-LTL showed highest total aromatics selectivity but most of the aromatics obtained were benzene and toluene, which result from hydrogenolysis of C8-aromatics [22]. Pt/SiO_2 showed highest selectivity to C8-aromatics, mostly *o*-xylene and ethylbenzene. Pt/K-BEA and Pt/K-MAZ also resulted in higher C8-aromatics than Pt/K-LTL. Pt/K-FAU as well as Pt/K-LTL resulted in hydrogenolysis of C8-aromatics.

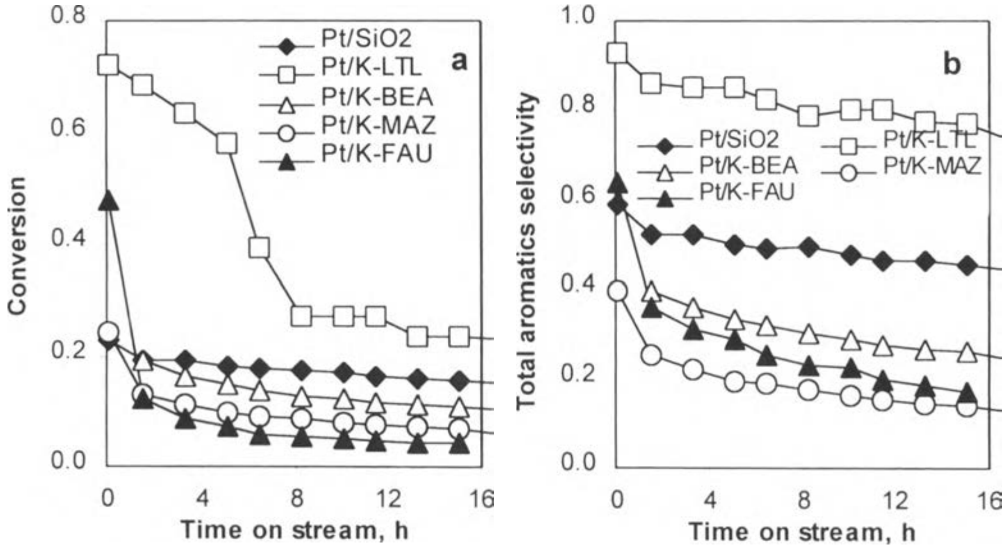

Fig. 3. (a) *n*-Octane conversion and (b) Total aromatics selectivity (mole basis) vs. time on stream over Pt/SiO_2 and Pt/zeolite catalysts. Reaction conditions: 500°C, H_2/*n*-C6 (or *n*-C8) molar ratio 6:1,WHSV 5 h^{-1}.

TABLE 3

Product distribution of *n*-octane aromatization on Pt/SiO_2 and Pt/zeolite catalysts, after 10 h on stream. Reaction conditions; 500°C, H_2: *n*-C8 ratio 6:1, WHSV 5 h^{-1}

	Pt/SiO_2	**Pt/K-LTL**	**Pt/K-BEA**	**Pt/K-MAZ**	**Pt/K-FAU**
Conversion Product selectivity (wt. %)	16.8	37.7	12.1	8.0	5.2
C1-C5	7.1	29.4	10.3	19.8	39.8
C6enes	4.3	1.2	5.1	6.7	9.7
C7enes	34.8	0.6	29.5	33.4	13.0
C8enes	5.4	1.9	25.6	23.5	17.7
Benzene	0.0	27.7	0.1	1.7	9.2
Toluene	0.9	28.2	1.8	2.1	4.5
EB	21.5	6.5	0.8	1.4	0.0
m-, *p*-Xylenes	1.5	1.4	14.5	5.5	3.7
o-Xylene	23.8	3.0	11.4	4.8	1.3
Total Aromatics	**47.8**	**66.8**	**28.6**	**15.4**	**18.7**
Total C8-aromatics	46.9	10.9	26.7	11.6	5.0
Total Olefins	44.5	3.7	60.2	63.6	40.3

Characterization of Spent Catalysts: All spent catalysts were analyzed by temperature programmed oxidation to study the nature and amount of coke deposit during the reaction. The TPO profiles of coke deposit on different catalysts are reported in Fig. 4. The weight percent of coke deposit on Pt/SiO_2, Pt/K-LTL, Pt/K-BEA, Pt/K-MAZ, and Pt/K-FAU are 0.87, 1.51, 1.92, 0.92, and 8.30, respectively. Iglesia *et al.* [27, 28] have shown that in the *n*-hexane aromatization reaction, the platinum that is well-dispersed inside the channels of the L zeolite is protected from bimolecular collision which leads to coke formation. The spent Pt/K-FAU catalyst exhibited much more coke deposit than other zeolite catalysts. It is possible that structure of FAU, which is 3-dimensional pore system, might be favorable to induce bimolecular collision, which is the cause of coke formation.

As described previously, Pt clusters can accelerate the oxidation of coke. Therefore, the coke oxidized at low temperature is located next to Pt cluster. In contrast, the high-temperature band (300-650°C) is possible due to the plugging of zeolite pores [22], which would retard the oxidation of the coke deposits. From the figure, BEA and MAZ spent catalysts exhibited only low-temperature peak similar to coke deposited on Pt/SiO_2. It is possible that Pt clusters over K-BEA and K-MAZ are mostly outside the zeolite channel and the reactions occurred on these platinum clusters leading to coke deposit outside the zeolite channel.

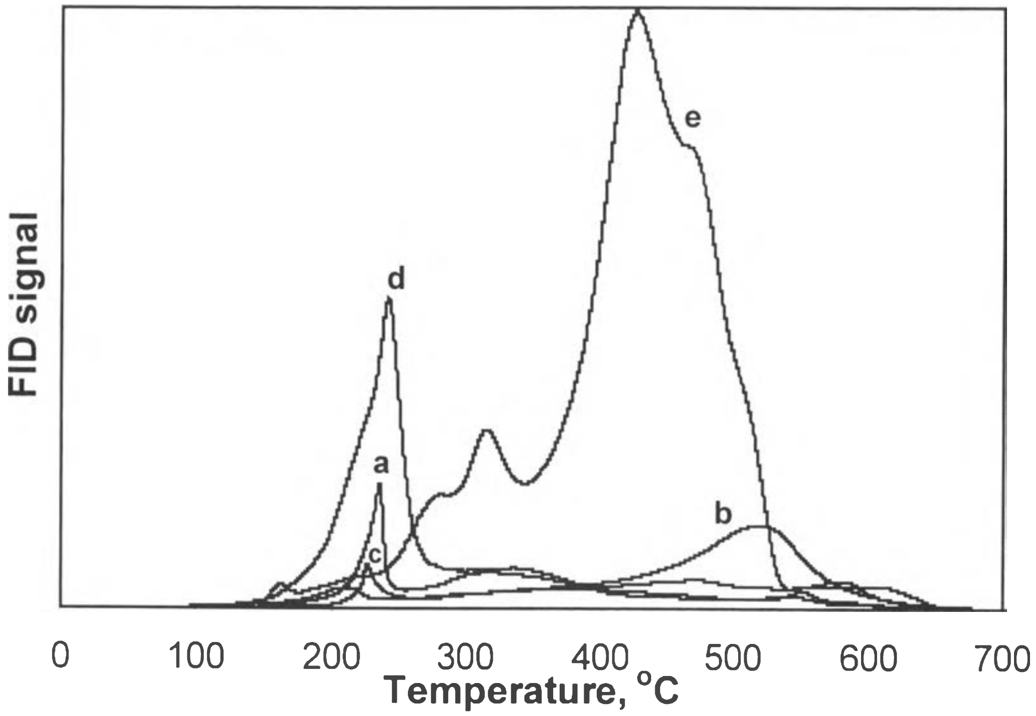

Fig. 4. TPO profiles of coke deposits on (a) Pt/SiO_2, (b) Pt/K-LTL, (c) Pt/K-BEA, (d) Pt/K-MAZ, and (e) Pt/K-FAU, after reaction at 500°C for 10 h on stream.

DISCUSSION

Similar to the studies of *n*-hexane aromatization, Pt/K-LTL is unique for *n*-octane aromatization among nonacidic large pore zeolite catalysts. In a previous study [7], it was found that the Pt/K-MAZ, which is structurally similar to Pt/K-LTL (unidimensional pore system, aperture of 7.1 A° for LTL and 7.4A° for MAZ) exhibited only little lower activity and benzene selectivity for the aromatization of *n*-hexane than Pt/K-LTL. However, in this work the Pt/K-MAZ exhibited much poorer ability than Pt/K-LTL for the aromatization of *n*-octane. At 10 h on stream, Pt/K-MAZ resulted in 15% aromatics with 8% conversion while Pt/K-LTL exhibit 66% aromatic with 38% conversion (see Table 3). H/Pt ratio after reduction at 500°C indicates that Pt/K-MAZ is one-sixth active platinum surface compared to Pt/K-LTL (see Table 2). Moreover, the results from DRIFTS of adsorbed CO demonstrate that Pt clusters on K-MAZ are located outside the zeolite leading to low total aromatics selectivity. In addition, Pt/K-BEA in which the structure is two-dimensional pore system with aperture of 6.7A° also exhibited Pt cluster outside zeolite channel resulting in low activity and total aromatic selectivity than Pt/K-LTL. The TPO results indicate that the activity and selectivity to aromatics of Pt/K-FAU dropped significantly due to coke formation. This might be because the structure of FAU, which is 3-dimensional pore system favors to induce bimolecular collision causing coke formation. Also, the results from TPD of ammonia indicated strong acid sites of this catalyst. These acid sites resulted in considerable cracking C1-C5 products (see Table 3). Like Pt/K-LTL, for *n*-octane aromatization, Pt/K-FAU resulted in hydrogenolysis aromatics which are benzene and toluene. These kinds of products were not found on the nonmicroporous and non-acid Pt/SiO_2 catalysts (see Table 3). This would indicate that the reactions over Pt/K-FAU as well as Pt/K-LTL occur inside the zeolite channel.

CONCLUSIONS

Among the Pt-containing large pore zeolites studied in this work, the Pt/K-LTL catalyst still. exhibits superior performance for the aromatization of *n*-octane. Even though the aperture size of MAZ is larger than LTL, the Pt/K-MAZ exhibited much lower activity and selectivity to aromatics than Pt/K-LTL. Pt dispersion and location are important factors to the aromatization performance. The uniqueness of Pt/K-LTL is due to the stability of Pt clusters in zeolite channels under reduction conditions. The structure and acidity of zeolite also affect product distribution and coke formation.

ACKNOWLEDGEMENTS

This work was supported by The Thailand Research Fund (TRF) under the Royal Golden Jubilee Ph.D. program and basic research project. Part of the experimental work was supported by the Oklahoma Center for the Advancement of Science and Technology (OCAST). We also thank the technical support of the personnel at the Petroleum Authority of Thailand (PTT) for the TPD experiment.

REFERENCES

1 Bernard, J. R., Proceedings in Fifth International Conference on Zeolite, L. V. C. Rees (Ed.), Heyden, London 686 (1980).

2 Hughes, T. R., Buss, W. C., Tamm, P.W., Jacobson, R. L., *Stud. Surf. Sci. Catal.* **28** 725 (1986).

3 Hughes, T.R., Mohr, D. H., Willson, C. R., *Stud. Surf. Sci. Catal.* **38** 335 (1987).

4 Law, D.V., Tamm, P. W., Detz, C. M., AIChE Meeting, Houston, TX, USA, March 29, 1987.

5 Besoukhanova, C., Breysse, C. M., Bernard, J. R., Barthomeuf. D., Catalyst Deactivation 201 (1980).

6 Hughes, T. R., Buss W. C., Tamm, P. W., Jacobson, R. L., AIChE Meeting, New Orleans, LA, USA, April 8, 1986.

7 Miller, J. T., Agrawal, N. G. B., Lane, G. S., Modica, F. S., *J. Catal.* **163** 106 (1996).

8 Jentoft, R. E., Tsapatsis, M., Davis, M. E., Gate, B. C., *J. Catal.* **179** 565 (1998).

9 Tauster, S. J., Steger, J. J., *J. Catal.* **125** 387 (1990).

10 Miller, J. T., Koningsberger, D. C., *J. Catal.* **162** 209 (1996).

11 Menacherry, P. V. and haller G. L., *J. Catal.* **177** 175 (1998).

12 Fukunaga, T. and Ponec, V., *J Catal.* **157** 550 (1995).

13 Derouane, E. G. and Vanderveken, D. J., *Appl. Catal.* **45** L15 (1988).

14 Fang, X., Li, F., Zhou, O., Luo, L., *Appl. Catal.* **161** 227 (1997).

15 Fang, X., Li, F., and Luo, L., *Appl. Catal.* **146** 297 (1997).

16 Jacobs, G., Alvarez, W. E., and Resasco, D. E., *Appl. Catal.* **206** 267 (2001).

17 Jongpatiwut, S., Sackamduang, P., Rirksomboon, T., Osuwan, S., Alvarez, W. W., and Resasco, D. E., *Appl. Catal.* , **230** 177 (2002).

18 Jacobs, G., Padro, C. L., and Resasco, D. E., *J. Catal.* **179** 43 (1998).

19 Jacobs, G., Ghadiali, F. , Pisanu, A., Padro, C. L., Borgna, A., Alvarez, W. E., and Resasco, D. E., *J. Catal.* **191** 116 (2000).

20 Jacobs, G., Ghadiali, F. , Pisanu, A., Borgna, A., Alvarez, W. E., and Resasco, D. E., *Appl. Catal.* **188** 79 (1999)

21 Ostgard, D. J., Kustov, L., Poeppelmeier, K. R., and Sachtler, W. M. H., *J. Catal.* **133** 342 (1992).

22 Jongpatiwut, S., Sackamduang, P., Rirksomboon, T., Osuwan, S., and Resasco, D. E., Submitted to *J. Catal.*, April 2002.

23 Fung, S. C., Querini, C. A., *J. Catal.* **138** 240 (1992).

24 Mielczarski, W., Hong, S. B., Davis, R. J., and Davis, M. E., *J. Catal.* **134** 359 (1992).

25 Hong, S. B., Mielczarski, W., and Davis, M. E., *J. Catal.* **134** 349 (1992).

26 Ballatreccia, M., Zanonin, R., Dossi, C., Psaro, R., Recchia, S., and Vlaic, G., *J. Chem. Soc. Farad. Trans.* **91** 2045 (1995).

27 Iglesia, E., Baumgartner, J. E., Proc. IX Internat. Zeolite. Conf., Montreal (1992).

28 Iglesia, E., Baumgartner, J. E., Proc. X Internat Congr. Catal. (Guczi L. *et al.*, Ed) p. 993, Elsevier Sci. Publ., New York (1993).